Kerr-induced Rotation of Mixed Orbital Angular Momentum States in Hollow Ring-Core Fibers

Sai Kanth Dacha[1,*], Wenqi Zhu[2], Amit Agrawal[2], Thomas E. Murphy[1]

[1] *Institute for Research in Electronics and Applied Physics (IREAP), University of Maryland, College Park*
[2] *National Institute of Standards and Technology (NIST), Gaithersburg, Maryland*
[*] *sdacha@umd.edu*

Abstract: We experimentally demonstrate that in the presence of Kerr nonlinearity, the spatial pattern caused by unequal excitation of two degenerate spin-orbit anti-aligned modes in an optical fiber exhibits a power-dependent rotation effect.

1. Introduction

Light beams carrying orbital angular momentum (OAM) are characterized by spiral phase distributions that can be expressed as $e^{iL\phi}$, where ϕ is the polar angular coordinate and L is an integer known as the topological charge. Each photon in such a light beam carries an orbital angular momentum equal to $L\hbar$ [1]. A mixed OAM state is a coherent combination of two or more OAM beams with different topological charges [2], and in general, has an average topological charge that is a non-integer [3]. In this work, we focus purely on a combination of fiber OAM modes with topological charges of equal magnitude and opposite sign.

OAM-carrying beams have recently received considerable attention owing to their applications in a wide variety of fields such as particle trapping and optical tweezers [4], classical and quantum communications [5], sensing [6] and quantum optics [7]. In the context of fiber optic communication, there is growing interest in using OAM-supporting fibers for space-division multiplexing (SDM) applications. Vortex fibers with tailored refractive index profiles have been shown to achieve stable linear propagation of OAM modes with minimal linear coupling among the spatial modes [8].

From a data transmission perspective, like in other types of multimode fibers, intermodal nonlinear effects in vortex fibers will play an important role in achieving SDM transmission over long distances [9]. To date, however, there have only been few studies reporting intermodal nonlinear interactions in vortex fibers. In this work, we demonstrate using experimental measurements Kerr nonlinearity-induced rotation of a superposition of two OAM modes propagating in a hollow ring-core vortex fiber.

2. Theory and Experiment

The electric field distribution of light in a vortex fiber can be equivalently described using the vector hybrid HE-EH mode basis as well as the vector OAM mode basis. The OAM modes can be expressed in terms of the hybrid modes as follows: $\vec{V}^{\pm L}_{SOa} = (\vec{HE}^{e}_{L+1} \pm i\vec{HE}^{o}_{L+1})/\sqrt{2}$ and $\vec{V}^{\pm L}_{SOaa} = (\vec{EH}^{e}_{L-1} \pm i\vec{EH}^{o}_{L-1})/\sqrt{2}$, where the superscript $e(o)$ denotes the even (odd) hybrid mode, and $\vec{V}^{\pm L}_{SO(a)a}$ denotes the spin-orbit (anti-)aligned modes of topological charge $\pm L$. Note that the term "spin-orbit (anti-)aligned" denotes the fact that the OAM and spin angular momentum (SAM), i.e. polarization, are (anti-)aligned. Here, we focus purely on the anti-aligned modes.

If E_1 and E_2 respectively denote the slowly-varying complex pulse envelopes of the $\vec{EH}^{e}$ and $\vec{EH}^{o}$ modes of the vortex fiber, the coupled nonlinear Schrödinger equations are (NLSEs) written as [10]:

$$\frac{\partial E_1}{\partial z} = iC_{1111}\left(|E_1|^2E_1 + \frac{2}{3}|E_2|^2E_1 + \frac{1}{3}E_2^2E_1^*\right), \quad and \quad \frac{\partial E_2}{\partial z} = iC_{2222}\left(|E_2|^2E_2 + \frac{2}{3}|E_1|^2E_2 + \frac{1}{3}E_1^2E_2^*\right) \tag{1}$$

where C_{jjjj} is the SPM coefficient corresponding to E_j. Upon converting Eqs. 1 to the OAM mode basis and making use of the fact that $C_{1111} = C_{2222}$ because the $\vec{EH}^{e/o}$ modes have identical intensity profiles, we obtain:

$$\frac{\partial V^+}{\partial z} = \frac{2i}{3}C_{1111}\left(|V^+|^2 + 2|V^-|^2\right)V^+, \quad and \quad \frac{\partial V^-}{\partial z} = \frac{2i}{3}C_{1111}\left(|V^-|^2 + 2|V^+|^2\right)V^- \tag{2}$$

where $V^{\pm}$ denote the slowly-varying complex pulse envelopes of the $\vec{V}^{\pm L}_{SOaa}$ modes. Eqs. 2 shows that the only third-order nonlinear terms that survive are the SPM and intermodal XPM terms, describing a power-dependent phase difference between the two modes.

Note that Eqs. 1 are identical to the coupled NLSEs for x and y polarization states in a single-mode fiber (SMF), while Eqs. 2 are identical to those obtained upon transforming the coupled NLSEs in SMFs from linear polarization basis to the circular polarization basis [11]. In the SMF case, these equations lead to the well-known

nonlinear polarization rotation effect, wherein the orientation of an elliptically polarized state exhibits a power-dependent rotation. When the input beam consists of short pulses, this leads to a time-dependent rotation of polarization ellipse. As a result, when averaged over the entire pulse duration, an apparent "depolarization" effect is observed where the time-averaged degree of polarization decreases with an increase in input power [11]. It must be noted that the nonlinear polarization rotation in SMFs is only observable for an elliptical state of polarization (i.e. an unequal superposition of the right and left circular polarizations).

OAM modes in fibers exhibit a similar effect, only with the added dimension of space. In the context of coupled NLSEs described in Eqs. 1 and Eqs. 2, the *HE-EH* mode basis is analogous to the x and y polarization basis in SMFs, while the OAM mode basis is analogous to the circular polarization basis. In an SMF, an unequal mixture of the right and left circularly polarized components leads to elliptical polarization. Here, as shown in Fig. 1(c), an unequal mixture of the $L = +10$ and $L = -10$ SO_{aa} modes yields a spatially non-uniform distribution of elliptical polarization with each spatial point on the beam having an elliptical state of polarization with the same ellipticity but the orientation of the ellipses varies in the azimuthal direction.

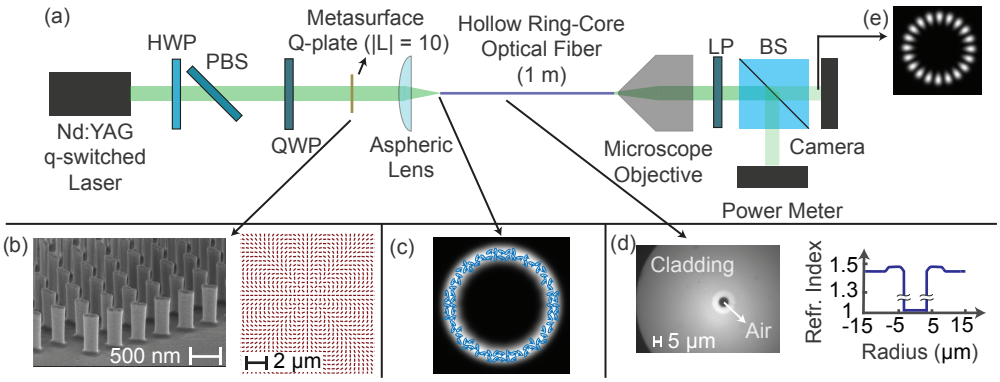

Fig. 1. (a) Experimental Setup for Characterizing Nonlinear Rotation of OAM States, (b) Metasurface q-plate design showing individual nanopillars and a schematic of their layout, (c) Vector mode profile for the mode mixture $\vec{V}_{SOaa}^{+10} + 0.2\vec{V}_{SOaa}^{-10}$, (d) Optical micrograph of hollow ring-core vortex fiber and its cross-sectional refractive index profile, (e) Example lobe pattern that is observed for a mixed OAM state when imaged with a linear polarizer.

In SMFs, nonlinear polarization rotation occurs because of a power-dependent phase difference between left and right circularly polarized components arising from SPM and XPM. Similarly, for a superposition of $L = \pm 10$ SO_{aa} modes in a vortex fiber, SPM and XPM cause a power-dependent phase difference between the modes according to Eqs. 2. This results in a power-dependent rotation of the polarization ellipse at each spatial location across the *entire* beam. This can be equivalently described as a power-dependent rotation of the entire complex vector beam about the singularity at the center.

Fig. 1(a) shows a schematic of the setup for this experiment. We use a Nd:YAG laser that emits Gaussian pulses of 720 ps FWHM width. In order to tunably excite an unequal mixture of the $L = \pm 10$ SO_{aa} modes, we designed and fabricated a transmissive dielectric metasurface q-plate to implement the phase profile $\theta(r,\phi) = L\phi$ for LCP (or RCP), where r andϕ are the polar coordinates of the q-plate, and $L = \pm 10$. As shown in Fig. 1(b), the metasurface consists of a two-dimensional array of high aspect-ratio, amorphous-Si nanofins [12] in a Cartesian grid, with a pitch of 400 nm. Each nanofin unit cell functions as a half-wave plate at $\lambda = 1064nm$, with fixed length of 272 nm, width of 104 nm, and height of 760nm. The q-plate phase profile is imparted via rotation of each nanofin at a given polar coordinate (r,ϕ) by an angle $\alpha(r,\phi) = \theta(r,\phi)/2$, according to the geometric Pancharatnam-Berry (PB) phase [13]. The metasurface design based on the PB phase naturally provides opposite topological charge numbers for orthogonal circular polarization states. The power ratio in the $L = \pm 10$ modes is controlled by adjusting the ellipticity of polarization of the laser beam using a quarter-wave plate. This beam is then focused into the guiding core layer of a hollow ring-core vortex fiber Fig. 1(d). The vortex fiber was chosen instead of commercially available step-index or graded-index for its ability to stably propagate OAM modes with minimal linear coupling between the modes [8, 14].

3. Results

When the output beam is imaged through a linear polarizer using a "slow" camera that averages over multiple pulse durations, patterns showing $2|L| = 20$ lobes are observed as shown in Fig. 1(e). The lobes arise from the spatial non-uniformity in the orientation of local polarization ellipses across the beam. When a Gaussian pulse propagates

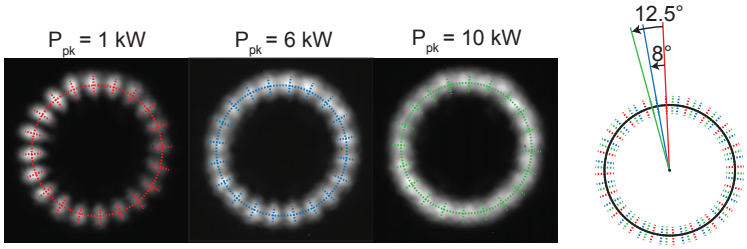

Fig. 2. Experimental measurements showing Kerr-induced power-dependent rotation of the output intensity profile when imaged through a linear polarizer

through the fiber in this configuration, the power-dependent rotation of the spatial distribution described above translates to a *time*-dependent rotation the entire pattern within one pulse duration. The time-dependent rotation of the entire vectorial spatial pattern is observed as a time-dependent rotation of the intensity pattern emerging from the linear polarizer. The time-dependent rotation that occurs within one pulse duration is still observed upon averaging over the entire pulse duration, as shown in Fig. 2. This is because the instantaneous orientation of the lobe pattern at the pulse peak is rotated relative to the lobe pattern at the pulse tails. Furthermore, we also observe a smearing out of the lobe pattern arising from the time-averaging. This is in direct analogy with the "depolarization" effect that occurs when characterizing the nonlinear polarization rotation effect in SMFs using time-averaged methods. These results were also validated using numerical simulations of Eqs. 2 (results not shown here).

It must be noted that the inhomogeneity in the polarization distribution across the beam as shown in Fig. 1(c) is essential for the observation of the lobe pattern following the linear polarizer. This, in turn, only occurs for an *unequal* mixture of $L = \pm 10$ $SO_{(a)a}$ modes. An equal mixture of the two modes is a true mode of the fiber as it is simply one of the EH modes, and therefore exhibits no power-dependent change in its pattern.

In conclusion, we demonstrated experimentally a novel power-dependent rotation phenomenon of a mixed OAM state consisting of an unequal admixture of the $L = \pm 10$ modes in a vortex fiber about its singularity. When observing a single point on the beam, this phenomenon holds similarities to the well-known nonlinear polarization rotation effect in SMFs where the local state of elliptical polarization rotates in a power-dependent manner. However, this effect can also be described as a power-dependent rotation of the entire complex vectorial beam about the on-axis singularity, which has no known analog in SMFs.

4. Acknowledgements

The authors would like to thank Siddharth Ramachandran's group (Boston University) for designing and OFS-Fitel LLC for manufacturing the hollow ring-core fiber used in this work.

References

1. L. Allen, M. W. Beijersbergen, R. J. C. Spreeuw, and J. P. Woerdman, Phys. Rev. A **45**, 8185 (1992).
2. Z. Bouchal, V. Kollarova, P. Zemanek, and T. Čižmár, Proc. SPIE - The Int. Soc. for Opt. Eng. **6609**, 83 – 90 (2007).
3. D. Preece, F. Flossmann, J. B. Götte, K. O'Holleran, M. J. Padgett, S. Franke-Arnold, and S. M. Barnett, Opt. Express, Vol. 16, Issue 2, pp. 993-1006 **16**, 993–1006 (2008).
4. D. G. Grier, Nat. 2003 424:6950 **424**, 810–816 (2003).
5. N. Bozinovic, Y. Yue, Y. Ren, M. Tur, P. Kristensen, H. Huang, A. E. Willner, and S. Ramachandran, Science **340**, 1545–1548 (2013).
6. M. P. Lavery, F. C. Speirits, S. M. Barnett, and M. J. Padgett, Science **341**, 537–540 (2013).
7. J. Leach, B. Jack, J. Romero, A. K. Jha, A. M. Yao, S. Franke-Arnold, D. G. Ireland, R. W. Boyd, S. M. Barnett, and M. J. Padgett, Science **329**, 662–665 (2010).
8. Z. Ma and S. Ramachandran, Front. Opt. Photonics pp. 213–228 (2021).
9. R. J. Essiambre, R. W. Tkach, and R. Ryf, Opt. Fiber Telecommun. VIB: Syst. Networks: Sixth Ed. pp. 1–43 (2013).
10. C. Antonelli, M. Shtaif, and A. Mecozzi, J. Light. Technol. **34**, 36–54 (2016).
11. G. Agrawal, "Nonlinear fiber optics," Nonlinear Fiber Opt. (2012).
12. W. R. McGehee, W. Zhu, D. S. Barker, D. Westly, A. Yulaev, N. Klimov, A. Agrawal, S. Eckel, V. Aksyuk, and J. J. McClelland, New J. Phys. **23**, 013021 (2021).
13. M. Khorasaninejad, W. T. Chen, R. C. Devlin, J. Oh, A. Y. Zhu, and F. Capasso, Science **352**, 1190–1194 (2016).
14. P. Gregg, P. Kristensen, and S. Ramachandran, Optica **2**, 267–270 (2015).